

## CHAPTER 25

### MASS TRANSPORT IN GRAVITY WAVES ON A SLOPING BOTTOM

by E.W.Bijker 1), J.P.Th.Kalkwijk 2) and T.Pieters 3).

#### Summary

In the present investigation the influence of bottom slope on mass transport by progressive waves was investigated, both theoretically and experimentally. Theoretical considerations based on linear wave theory show the greatest influence of the slope on the bottom drift velocities for relatively long waves and steep slopes. The numerical values, however, remain rather small (influence less than 20%). In addition, the experiments show that the bottom drift velocities are more determined by the local parameters than by the magnitude of the bottom slope in the cases examined. Considering the net bottom velocities, the discrepancy between the horizontal bottom theory (Longuet-Higgins) and experimental results is considerable. Taking into account the first harmonic of the local wave form and the small slope effect for relatively small depths in horizontal bottom theory does show, however, the same tendency as the experimental results.

#### 1. Introduction

The complexity of the mechanism of sediment movement under wave action makes the choice of the proper model bed material in coastal movable bed models often difficult. Therefore, a better knowledge of one of the details of this mechanism, namely the net mass transport in waves, would assist in determining the correct sediment scale or at least to recognize scale effects, if they are inevitable. Though the role of the mass transport velocity is not fully understood, experiments from past investigations suggest that it influences the near bottom and suspended sediment transport. Especially the influence of the beach slope on behaviour of this phenomenon in the model is then important, because of the frequently observed distortion in these models.

This paper reports results of experiments to determine mass transport velocities on three sloping bottoms. In particular attention was paid to the resultant bottom velocities, since those are most important for sediment studies. The considerations are limited to the off-shore region. Section 2 gives a brief survey of previous work. Section 3 aims at predicting the net bottom velocities as they occur on a gently sloping bottom; section 4 describes the various experiments carried out; sections 5 and 6 compare the experimental and theoretical results and give the conclusions.

#### 2. Review of previous work

Theoretical or experimental results for mass transport velocities over gently sloping bottoms are very scarce. Most investigations have

- 
- 1) Prof. of Coastal Engineering, Delft University of Technology, Department of Civil Engineering.
  - 2) Assoc. Prof. of Hydraulic Engineering, Delft University of Technology, Department of Civil Engineering.
  - 3) Student of Civil Engineering, Delft University of Technology.

been carried out with horizontal bottoms. In this connection Longuet-Higgins (1) has made a most important theoretical contribution. In his paper he gives solutions for very low waves (laminar boundary layer conduction solution). In these cases good agreement between theory and experiment was obtained for values of  $kh$  ( $k$  = wave number,  $h$  = water depth) between 0.9 and 1.5. Experiments for higher values of  $kh$  generally yielded a mass transport velocity profile resembling better the Stokes profile. This is reported in (2).

Despite of the fact that Russell and Osorio (3) carried out their experiments with higher waves, the tendencies predicted by Longuet-Higgins were confirmed. Though in most of their cases the boundary layer was turbulent, Longuet-Higgins showed in the appendix of their paper that, in particular, the velocity just outside the boundary layer at the bottom does not depend on the value of the (eddy) viscosity, provided it is constant. In general, it may be concluded, however, that the results for the high waves are less good than for the low waves.

Brebner, Askew and Law (4) examined the influence of roughness on the mass transport. In general, they found at the bottom a smaller velocity than predicted by Longuet-Higgins theory. They suggest that this is caused by the turbulent boundary layer. Noda (5) - using in his computations an eddy viscosity, being a function of distance from the wall {see also (6)} - attempted to explain this phenomenon, but he only found a significant effect for the case of standing waves. Sleath (7) attempted to explain the phenomenon by taking into account convective acceleration terms. His corrections (both positive and negative) amount to an order of 10% for the cases considered.

Another attempt of Sleath (8) to determine differences between Longuet-Higgins theory and experiments is based upon the introduction of damping waves in the longitudinal direction. His mathematical formulation yields three possible solutions for the Longuet-Higgins case (low waves). Unfortunately, it is not clear under which circumstances the various solutions hold. Moreover the experimental support is weak.

For a gently sloping bottom Russell and Osorio (2) observed for a single case considered, no significant differences from the results on a flat bottom. Lau and Travis (9) also considered a sloping bottom, but they were primarily interested in the consequences of partial reflection on mass transport velocity profiles.

Concluding, one may remark that net velocity profiles in physical models, although already very schematized, are not satisfactorily predicted by existing theories for cases with relatively high waves. In order to indicate tendencies at best, Longuet-Higgins theory can be used.

### 3. Theoretical considerations

In this section it is attempted to predict the behaviour of the net bottom velocities in progressive waves propagating on a gently sloping bottom. As a consequence of the latter limitation, partial reflection of the progressive waves will be disregarded.

A conventional  $x, z$  coordinate system is used as shown in figure 1 (page 4).

The following two-dimensional equation of motion holds for the boundary layer at the bottom (vertical velocity negligible):

$$\frac{\partial u}{\partial t} + u \frac{\partial u}{\partial x} + \frac{1}{\rho} \frac{\partial p}{\partial x} = \nu \frac{\partial^2 u}{\partial z^2} \quad \{1\}$$

In the following it will be also assumed that the velocity remains small, so that the convective acceleration terms in the equation{1} can be neglected. Furthermore, since in first order of approximation the fluid motion in the interior is not influenced by viscosity, the pressure gradient in the thin boundary layer at the bottom (assumed to be equal to the pressure gradient just outside the boundary layer) is also equal to the corresponding local acceleration, so:

$$\frac{1}{\rho} \frac{\partial p}{\partial x} = - \frac{\partial u_{\infty}}{\partial t} \quad \{2\}$$

and eqn.{1} changes into:

$$\frac{\partial u}{\partial t} - \frac{\partial u_{\infty}}{\partial t} = \nu \frac{\partial^2 u}{\partial z^2} \quad \{3\}$$

In the case under consideration (progressive waves) the horizontal fluid motion is given by {see (10) and (11)}:

$$u = A(x) \left[ \cos(\omega t - \phi(x)) - e^{-\frac{h+z}{\delta}} \cos\left(\omega t - \phi(x) - \frac{h+z}{\delta}\right) \right] \quad \{4\}$$

in which

$$\delta = \left( \frac{2\nu}{\omega} \right)^{\frac{1}{2}}$$

$$A(x) \cos(\omega t - \phi(x)) = u_{\infty}$$

$$\frac{\partial}{\partial x} \phi(x) = k(x)$$

The result for  $u$  can be conceived of as the first order result for the Eulerian velocity in the boundary layer. The time average of this result yields a zero net velocity. To determine the mean second order Eulerian velocity, the equations of motion have to be applied again. From the equation of continuity:

$$\frac{\partial u}{\partial x} + \frac{\partial w}{\partial z} = 0 \quad \{5\}$$

the small second order vertical velocities can be derived. This yields:

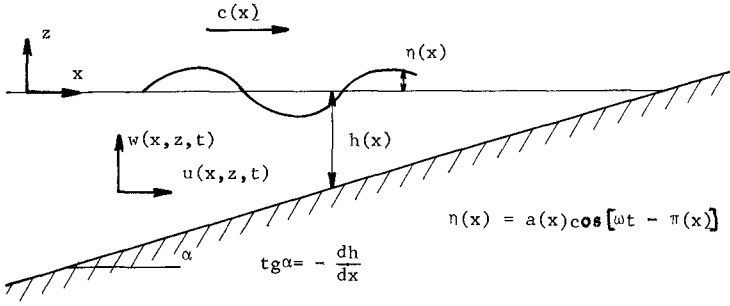


fig.1. Definition sketch

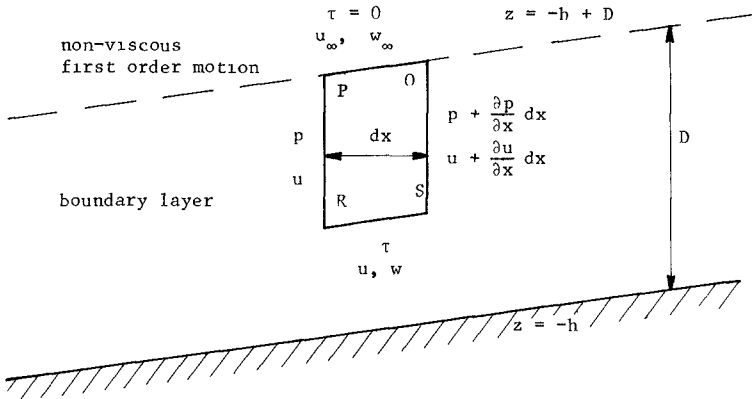


fig.2. Spatial fixed volume in boundary layer

$$\begin{aligned}
 w = & +A \delta k \left[ \left\{ \frac{1}{2} e^{-\mu} (\sin\mu + \cos\mu) - \frac{1}{2} \right\} \cos\psi + \left\{ -\mu + \frac{1}{2} e^{-\mu} (\sin\mu - \cos\mu) + \frac{1}{2} \right\} \sin\psi \right] \\
 & -\delta \frac{dA}{dx} \left[ \left\{ \mu - \frac{1}{2} e^{-\mu} (\sin\mu - \cos\mu) - \frac{1}{2} \right\} \cos\psi + \left\{ \frac{1}{2} e^{-\mu} (\sin\mu + \cos\mu) - \frac{1}{2} \right\} \sin\psi \right] \\
 & -A \frac{dh}{dx} \left[ \{-e^{-\mu} \cos\mu + 1\} \cos\psi + \{e^{-\mu} \sin\mu\} \sin\psi \right] \quad \{6\}
 \end{aligned}$$

This complicated result is due to the fact that derivatives of A(x) and h(x) must be taken into account.

Application of the law of conservation of momentum to a spatial fixed element (P Q R S in figure 2, page 4) yields:

$$\frac{\partial}{\partial t} \iiint_V \rho u \, dV = \{\rho uw\}_x dx - \{\rho uw\}_\infty dx + \tau \, dx - \int_z^{-h+D} \frac{\partial}{\partial x} \left( \frac{p}{\rho} + u^2 \right) dx \, dz \quad \{7\}$$

Taking the time average yields:

$$v \frac{\partial \hat{u}}{\partial z} = \{\overline{uw}\} - \{\overline{uw}\}_\infty - \int_z^{-h+D} \frac{\partial}{\partial x} \left( \frac{\bar{p}}{\rho} + \overline{u^2} \right) dz \quad \{8\}$$

so that:

$$\bar{u} = \frac{1}{v} \int_{-h}^z (\{\overline{uw}\} - \{\overline{uw}\}_\infty) dz - \frac{1}{v} \int_{-h}^z \int_z^{-h+D} \frac{\partial}{\partial x} \left( \frac{\bar{p}}{\rho} + \overline{u^2} \right) dz \, dz \quad \{9\}$$

since the left member of eqn. {7} is then equal to zero. The pressure term in eqn. {9} will again be derived from the interior of the fluid. Taking the time average of the governing equation of motion (neglecting viscous terms) yields:

$$\frac{1}{\rho} \frac{\partial}{\partial x} \bar{p} = -\frac{1}{2} \frac{\partial}{\partial x} \overline{u^2} - \overline{w \frac{\partial}{\partial z} u} \quad \{10\}$$

and at the bottom (w = 0):

$$\frac{1}{\rho} \frac{\partial}{\partial x} \bar{p} = -\frac{1}{2} \frac{\partial}{\partial x} (\bar{u}_{\infty}^2) \quad \{11\}$$

Physically the gradient of the time mean pressure arises from the variation of the mean water level.

After substituting {4}, {6} and {11} in {9} the mean value  $\bar{u}$  can be calculated:

$$\begin{aligned} \bar{u} = & \frac{A^2 k}{\omega} \left[ -\frac{1}{2} e^{-\mu} \{ \sin \mu + \cos \mu \} + \frac{1}{2} e^{-\mu} \sin \mu - e^{-\mu} \cos \mu + \frac{1}{4} e^{-2\mu} + \frac{3}{4} \right] \\ & + \frac{A}{\omega} \frac{dA}{dx} \left[ \frac{1}{2} e^{-\mu} \{ \sin \mu - \cos \mu \} + 2e^{-\mu} \sin \mu + \frac{1}{2} e^{-\mu} \cos \mu + \frac{1}{4} e^{-2\mu} - \frac{3}{4} \right] \end{aligned} \quad \{12\}$$

The result obtained is the Eulerian mean velocity. The mean particle velocity (Langrangian velocity) can be derived using the relation:

$$\bar{U} = \bar{u} + \overbrace{\frac{\partial u}{\partial x} \int u dt}^t + \overbrace{\frac{\partial u}{\partial z} \int w dt}^t \quad \{13\}$$

Using the results obtained from  $u$  and  $w$ , the remaining unknown terms in the right member of eqn. {10} yield:

$$\begin{aligned} & \overbrace{\frac{\partial u}{\partial x} \int u dt}^t + \overbrace{\frac{\partial u}{\partial z} \int w dt}^t = \\ & = \frac{A^2 k}{\omega} \left[ \frac{1}{2} e^{-\mu} \{ \sin \mu + \cos \mu \} - \frac{1}{2} e^{-\mu} \sin \mu - e^{-\mu} \cos \mu + \frac{1}{2} e^{-2\mu} + \frac{1}{2} \right] + \\ & + \frac{A}{\omega} \frac{dA}{dx} \left[ -\frac{1}{2} e^{-\mu} \{ \sin \mu - \cos \mu \} - \frac{1}{2} e^{-\mu} \cos \mu + \frac{1}{2} e^{-2\mu} \right] \end{aligned} \quad \{14\}$$

Eqs. {12} and {14} substituted in eqn. {13} gives the result desired:

$$\bar{U} = \frac{A^2 k}{\omega} \left[ -2e^{-\mu} \cos \mu + \frac{3}{4} e^{-2\mu} + \frac{5}{4} \right] + \frac{A}{\omega} \frac{dA}{dx} \left[ 2e^{-\mu} \sin \mu + \frac{3}{4} e^{-2\mu} - \frac{3}{4} \right] \quad \{15\}$$

and at the edge of the boundary layer:

$$\bar{U}_{\infty} = \frac{5}{4} \frac{A^2 k}{\omega} - \frac{3}{4} \frac{A}{\omega} \frac{dA}{dx} \quad \{16\}$$

The first term in expression {15} is the same as derived by Longuet-Higgins for progressive waves on a horizontal bottom. The dimensionless expression between brackets in the second term, giving the distribution in the boundary layer, is the same as derived for a standing wave. It should be stressed however, that this result holds for progressive waves with varying amplitude, caused for example by a gently sloping bottom.

Both dimensionless functions between brackets are also given in (1), (5) and (6), where in the two latter publications both laminar and turbulent boundary layers are considered.

Since A is the amplitude of the velocity at the bottom of the interior of the fluid (at the edge of the boundary layer) it can be expected to increase continuously in a progressive wave, propagating on the slope before breaking. Therefore, the first term of the right member of eqn. {16} (the Longuet-Higgins term) indicates a continuous increase of the net bottom velocity in a progressive wave, propagating over a constant slope. Subsequently, the derivative of A with respect to x, is positive in that case, so that the second term of the right member of eqn. {16} indicates a diminishing influence on the net bottom velocity as predicted by the Longuet-Higgins theory. An assessment of the influence of the latter term is possible by considering the transformation of a progressive wave propagating on a beach using the energy concept (linear theory). Then the expression for the amplitude of the oscillating bottom velocity is:

$$A = \hat{u}_\infty = \frac{a_0 \omega}{\sinh kh} \left[ \frac{2 \cosh^2 kh}{2kh + \sinh 2kh} \right]^{\frac{1}{2}} \quad \{17\}$$

This expression represents the influence of a varying water depth, but it does not contain derivatives with respect to x. Therefore, the influence of the correction term in eqn. {16} is proportional to the slope of the bottom. Normalizing the correction term with the Longuet-Higgins term yields for  $\bar{U}_\infty$  :

$$\bar{U}_\infty = \frac{5}{4} \frac{A^2 k}{\omega} \left[ 1 - \frac{3}{5} \frac{1}{Ak} \frac{dA}{dh} \frac{dh}{dx} \right] \quad \{18\}$$

For a constant slope the dimensionless correction term is a function of  $k_0 h$  (or  $kh$ ), only, and is graphically represented in fig.3, page 8. The figure shows that in general the influence of the correction term is small. Its influence is greatest for the relatively long waves; or, in other words, near the breaker zone. Under practically all conditions its value will remain below 0.2, for slopes up to 1:10. It is also very doubtful whether the linear wave theory can be applied to the breaker zone. The shallower the water, the more important the non-linear effects. Due to shoaling, for instance, the waves obtain a very pronounced crest and flat trough. The corresponding velocity at the bottom will behave the same, and in fact higher harmonics must be taken into account then. If these harmonics have the same celerity, ref.(3) indicates how to take them into account:

$$\bar{U}_\infty = \frac{5k}{4\omega} \left[ A_1^2 + A_2^2 + \dots \dots \dots \right] \quad \{19\}$$

in which  $A_1, A_2 \dots$  are the amplitudes of the bottom velocities due to the various harmonics.

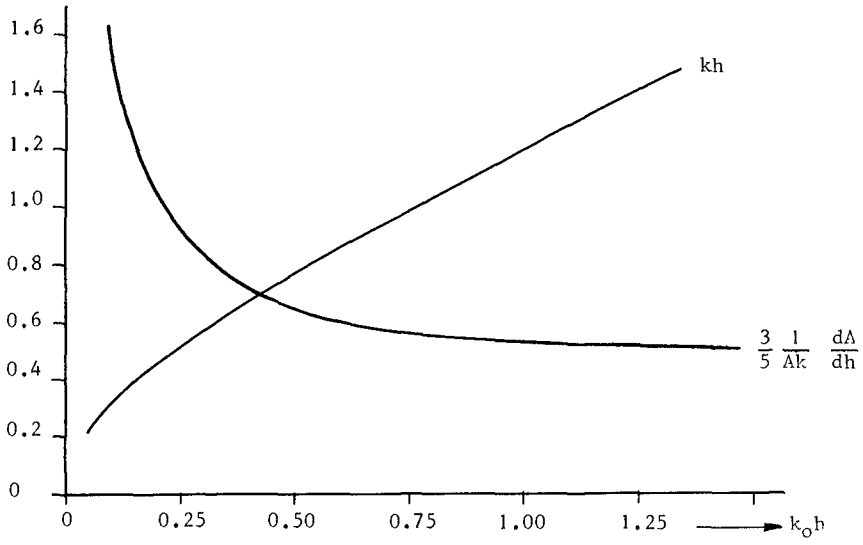


fig.3. Slope effect according to eqn.18

4. Experiments

4.1. General remarks

Experiments were carried out in a wave flume, 30 m long, 0.80 m wide and 0.60 m deep. Waves were generated by a wave-paddle, oscillating with different amplitudes - if necessary - at the bottom and still water levels (see fig.4, page 10).

Three different beach slopes were used, viz. 1:10, 1:25 and 1:40. The slope surface was rigid, whereas its roughness was varied, viz. painted smooth concrete, glued sand grains and artificial ripples. The diameter of the sand grains was between 1.6 and 2.0 mm; length and height of the symmetrical ripples were 80 mm and 18 mm, respectively. The water depth in front of the beaches ( $h_h$ ) was constant (0.45 m). During all experiments wave profiles over the full length of the flume were recorded and the data were analyzed by means of Fourier-analysis. In this way the character of the waves and their behaviour on the beaches (higher harmonics, position and nature of breaking, etc.) were determined. Furthermore, disturbances to the mass transport, such as caused by reflection, seiches and free higher harmonics, could be distinguished.

Table I gives a survey of the data of the waves, used in the experiments:

number of the wave	T in sec.	$H_o$ in m	$H_o/L_o$	$H_h/L_h$	$k_h h_h$
1	1.0	0.094	0.058	0.060	1.88
3	1.5	0.043	0.010	0.015	1.04
4	1.5	0.095	0.026	0.033	1.04
5	1.5	0.181	0.046	0.059	1.04
7	2.0	0.095	0.014	0.023	0.72

TABLE I Initial wave properties

The waves, before reaching the beach, agreed very well with the second order Stokes wave form (see table II).

All waves applied broke on the beaches. The reflection was always less than 6%. In all experiments the amplitude of the free second harmonic component did not exceed 12% of the value of the first harmonic.

number of the wave	$a_1$ in m	$\frac{a_1}{a_1 \text{ refl. in } \%}$	$\frac{a_1}{a_2}$	theor. $\frac{a_1}{a_2}$ (Stokes)	$\frac{a_2 \text{ free } a_1 \text{ in } \%}{a_1}$
1	0.043	3.6	8.3	8.8	1.2
3	0.021	4.0	16.3	17.0	2.0
4	0.043	5.2	8.0	7.5	2.3
5	0.078	4.6	3.9	4.2	5.9
7	0.045	6.0	5.1	5.1	11.8

TABLE II Measured wave properties above the horizontal bottom in the front of the beaches.

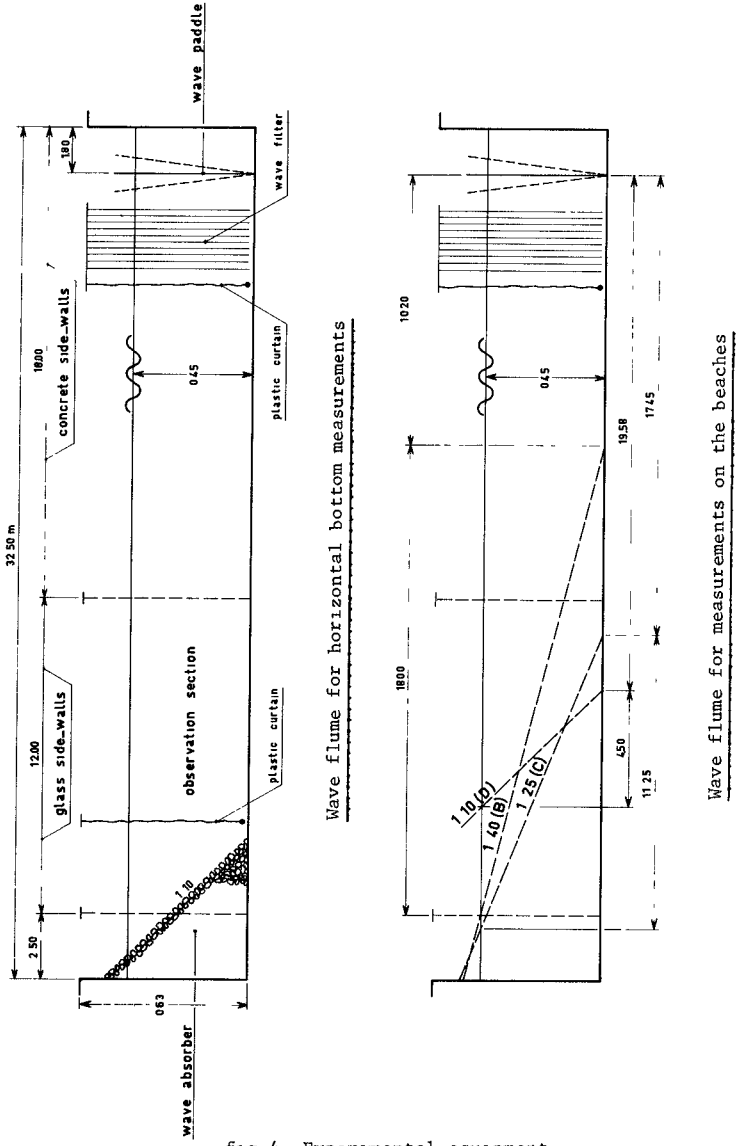


fig.4. Experimental equipment

The breaking behaviour of the waves was usual; with increasing beach slope the form of breaking changed from spilling to plunging and the breaker depth decreased.

Preliminary experiments with a horizontal bottom showed the necessity for taking special measures against disturbing influences; a plastic curtain was hung in front of the wave generator, to prevent drift currents induced by the machine, to enter the measuring section. The surface was kept clean by addition of a small amount of surface tension reducing agent.

To ensure that in all cases a steady state was reached, the wave generator was started 15 hours before making definite measurements. Some mass transport velocity profiles, recorded after only half an hour, did not show, however, significant differences with the final results.

#### 4.2. Measurements

The mass transport velocities were determined by filming small rigid particles, with about the same density (995-1005 kg/m<sup>3</sup>) as water, measuring the displacement during an integer number of wave periods and dividing by time. In this way mean particle velocity profiles were constructed for corresponding places (depths) on the various beaches (fig.5, page 12). This method of measurement is very time consuming. Direct measurement, using for instance, a current meter on a fixed location, however, is not possible, since this would yield the mean Eulerian velocity, whereas the resultant Lagrangian velocity is required. Because of the dimensions of the rigid particles (5 mm dia.), the measured velocities represent averaged values over at least the dimension of the grains. This averaging effect is greatest near the bottom, where the vertical gradient of the mass transport velocity is usually largest.

### 5. Discussion of results

#### 5.1. Preliminary experiments

These results with a horizontal bottom and those of Russell and Osorio (3) show similar agreement with the theory developed by Longuet-Higgins (1):

- the distribution over the depth was rather well predicted for the waves 3, 4 and 5 ( $k_h h_h = 1.04$ ), whereas the agreement became less for the waves 1 and 7 ( $k_h h_h = 1.88$  and  $0.72$ , respectively);
- the bottom velocities disagreed less than those at the surface;
- the predicted values, however, are mainly too large as compared with the measurements. This deviation becomes stronger with increasing wave amplitude.

On the basis of the rather good agreement with other experiments, it was decided to continue with the sloping bottoms.

#### 5.2. Sloping bottoms

##### 5.2.1. Smooth bottom

It is not possible to give all experimental results in this limited paper. Therefore, only a typical example of transport velocities

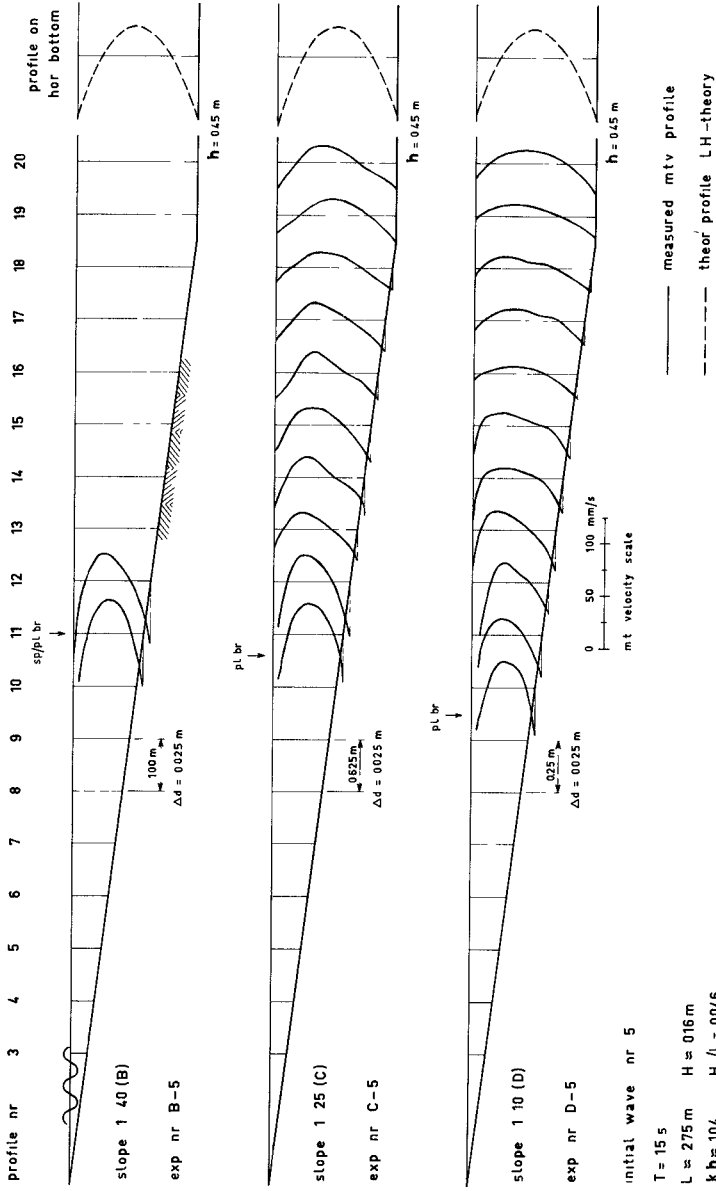


fig.5. Same initial wave on beaches with different slopes

for a smooth bottom is given in fig.5, page 12. Generally speaking, the tendencies shown by the experiments are confirmed by Longuet-Higgins theory. The latter predicts initially, for the case shown in fig.5, a forward flow at the bottom and at the surface, and a back flow in the center of the body of water. Approaching the beach the value of  $kh$  gradually decreases. As a consequence, the basic profile of the mass transport gradually changes into a shape where a back flow occurs at the surface. The latter, however, only occurs when steepness of the wave and relative water depth are small. The same phenomenon was also observed by Russell and Osorio (3). When the water depth becomes very small the surface velocities increase considerably. This was also in agreement with the results of Mei, et al.(2). The flume side walls may have an influence on the surface velocities, however. Therefore, the results for the deeper regions must be treated with some caution {see also (2)}.

The behaviour of the mass transport profile close to the breaker region is different. In that region the flow profile has the same shape for all waves, namely rather strong forward velocities at bottom and surface, with a back flow in between. There, the velocities could obtain values greater than predicted by Longuet-Higgins theory. In the breaker zone, the net bottom velocities were always directed toward deeper water. Differences in these velocities could not be distinguished, despite the fact that the waves on the various slopes could break in different ways (spilling or plunging).

Outside the breaker zone, the theoretical Longuet-Higgins values (based on local wave height) considerably exceeded the experimental values. This is shown in figures 6 and 7 (pages 14 and 15) in more detail. Both figs.6 and 7 give bottom velocities; in fig.6 the results are given for 3 waves with equal wave heights, but different periods over 3 different slopes. Fig.7 contains the results for a wave with constant period, but different heights, also propagating over 3 different slopes. The experimental bottom velocities in these figures are normalized by the theoretical Longuet-Higgins value determined using the local wave height. This might be an inconsistent way of normalizing, but the wave heights at the various slopes did not show great differences, provided the initial wave was the same. As a consequence, the values obtained are well comparable.

The scatter of the experimental data shown in the parts a and b of figures 6 and 7 is smaller than the reported values might indicate. This is caused by the method of normalizing applied to small velocities.

The solid curves in the figures, valid for the various slopes, were calculated by means of an averaging procedure applied to the non-dimensional measured values.

In these figures, the correction according to eqn. {18} (see also fig.3) for the 1:10-slope, is plotted using dotted curves. The correction based on eqn. {19}, in which only the experimental first harmonic is considered (practically the same for the various slopes with the same initial waves), is plotted in the same way. For a better comparison, in fact, the higher harmonics should be taken into account as well. Since these terms in eqn.{19} occur in quadratic terms, they are neglected here. In fact both influences have to be superimposed.

It can be concluded from the figures that the correction to the

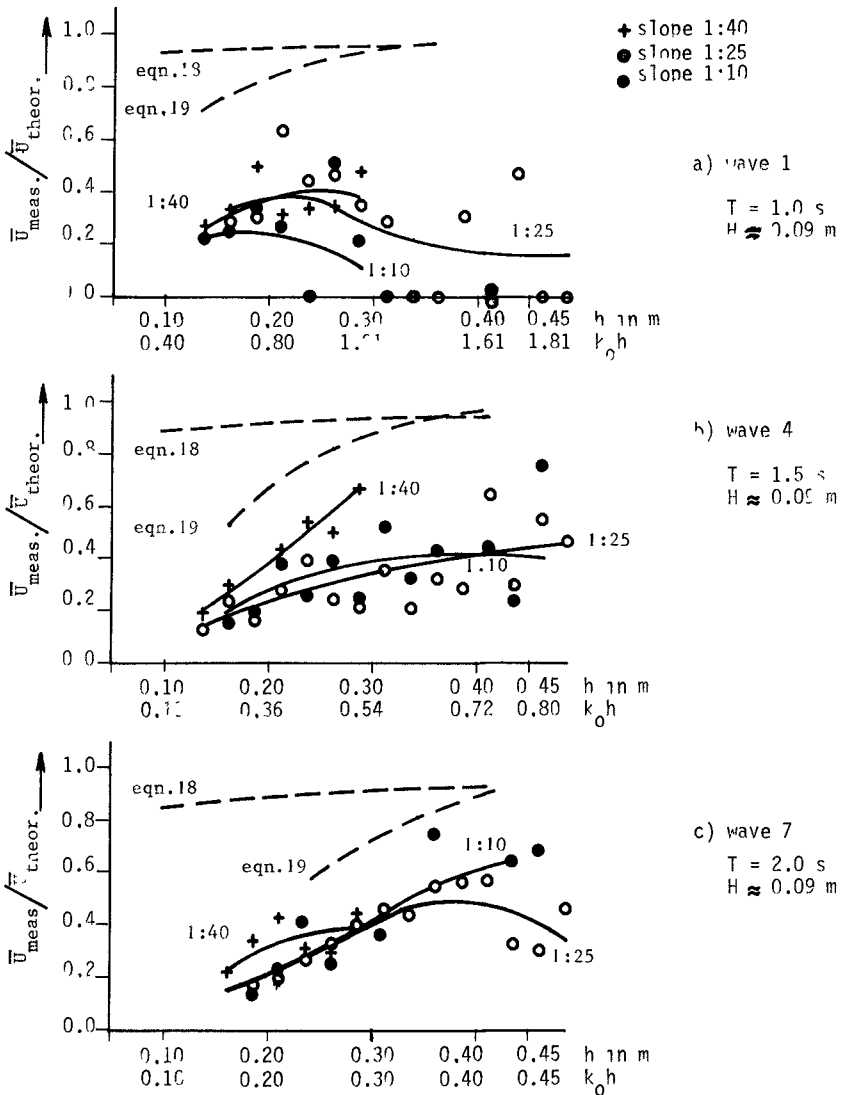


fig.6. Bottom drift velocities in waves with different periods

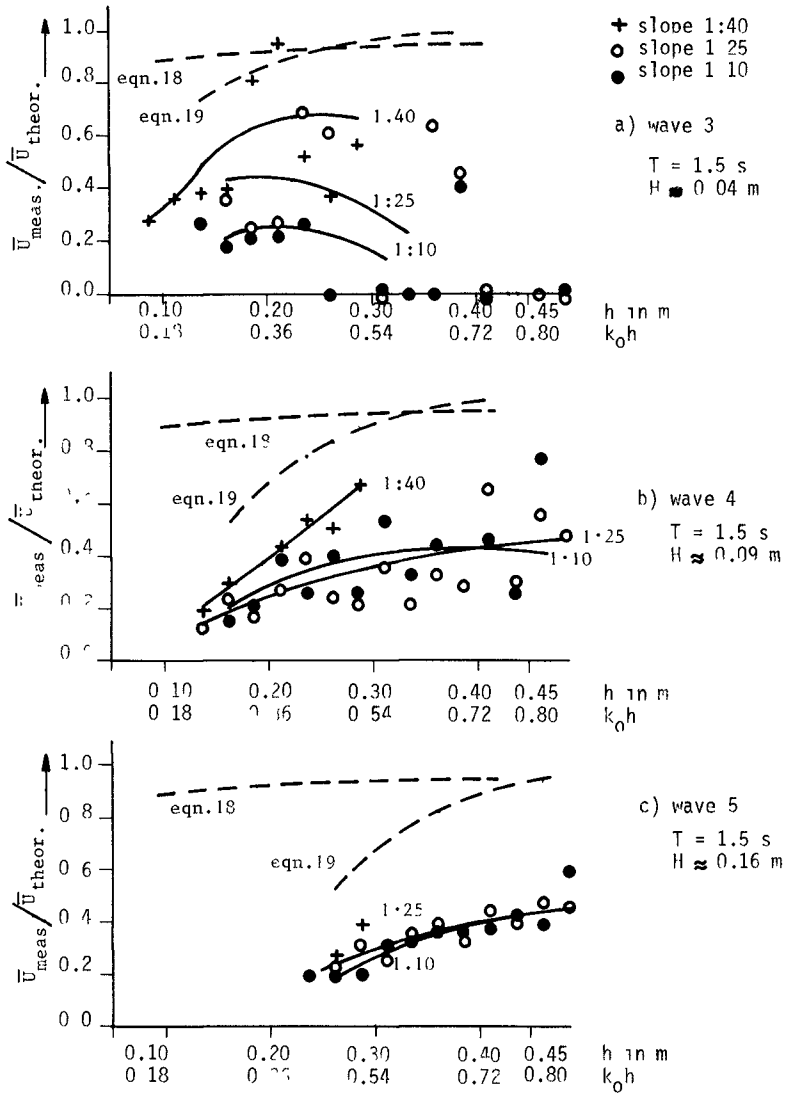


fig.7. Bottom drift velocities in waves with different heights

Longuet-Higgins values using the first harmonic is generally greater than the correction for slope. In the region where the corrections are most significant (small  $kh$  values), the former can be 3 times greater than the latter. Though both corrections diminish the theoretical values, they are always still greater than the experimental values. Nevertheless, the tendencies predicted by the corrections are confirmed by the experiments. Considering, for instance, fig.6, the corrections for the longest wave are greatest and this is rather well confirmed by the experiment. In fig.7 a similar behaviour of predicted and measured values can be observed.

The steepness of the slope does not seem to have a very significant influence on the bottom velocities. The 1:40 slope may show somewhat higher values; in general, the differences with the results for the other slopes are small.

Concluding, one can say that the bottom velocities are primarily determined by the local wave parameters, such as depth, height and shape of the wave. The gradient of the bottom has no significant influence. In the cases examined, distortion of the model has only minor consequences for these velocities. Although the distortions used in this model were not perfect (the initial water depth remained constant while the slope varied), there is enough experimental support for this conclusion {see also (3)}. It is also suggested that distortion of prototype situations with less steep slopes is permitted as far as bottom velocities are concerned. The explicit proof, however, has not been delivered.

#### 5.2.2. Rough bottom

The experiments with the slope surface with sand roughness show the same tendencies as mentioned before (see fig.8, page 17). The only difference compared to the smooth slope is that all velocities at comparable places are somewhat smaller, especially those at the bottom. The thickness of the layer, where the latter velocities occur, decreases slightly at corresponding places.

#### 5.2.3. Artificial ripples

The artificial ripples prove to have an important influence on the drift profile. The initially forward velocity at the bottom is reduced to about zero, whereas close to the bottom a consistent flow is induced. The direction of this current seems to depend on the wave steepness. Wave 3 ( $H_w/L_w = 0.015$ ) shows a forward velocity, whereas waves 4 and 5 ( $H_w/L_w = 0.033$ , resp. 0.059) show a strong backward current at the same level (fig.8, page 17). The consistency of the forward current (small wave steepness) seems to depend on the bottom slope. This phenomenon indicates the existence of a critical wave steepness for the reversal of this current between 0.033 and 0.015.

At this moment the amount of experimental data on rough bottoms like these, is not sufficient to draw general conclusions. The profiles observed, however, are so different from the smooth cases, that further investigations in this field are justified.

### 6. Conclusions

As far as it is permitted to draw general conclusions for the area

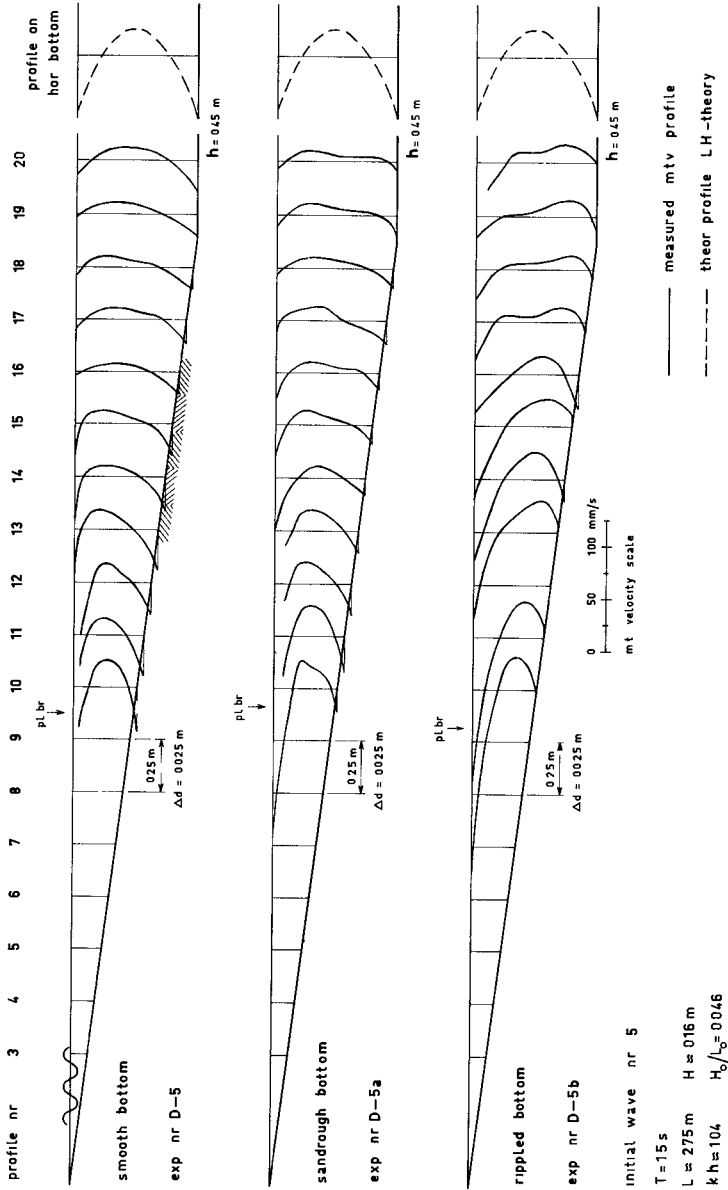


fig.8. Same wave on beaches with different bottom roughness (slope 1:10)

outside the breaker zone from this restricted number of experiments, it can be noted that:

- the bottom transport velocities on the slopes seem to be determined by the local depth rather than by the slope-angle;
- the bottom velocities predicted by the horizontal bottom theory are too large for the sloping bottom;
- the discrepancy between theory and experiment increases with decreasing depth and increasing relative wave length and wave height;
- the inclusion of the change in wave form and slope effect appears to explain the behaviour of the bottom velocities qualitatively;
- the drift velocities change slightly for increasing bottom roughness and considerably when a ripple-like roughness is present.

#### List of symbols

- a = amplitude of surface elevation  
 A = maximum orbital velocity at the bottom outside the boundary layer  
 c = wave phase celerity  
 D = boundary layer thickness
- $$\delta = \left( \frac{2\nu}{\omega} \right)^{\frac{1}{2}}$$
- h = local still water depth  
 H = wave height
- $$k = \frac{\partial \phi(x)}{\partial x} = \text{local wave number}$$
- L = wave length  
 p = normal pressure  
 t = time  
 T = the wave period  
 $\tau$  = shear stress  
 u = horizontal Eulerian velocity component  
 U = horizontal particle (Lagrangian) velocity component  
 w = vertical Eulerian velocity component
- $$\omega = \frac{2\pi}{T}$$
- x = horizontal coordinate  
 z = vertical coordinate  
 $\mu = (h+z)/\delta$   
 $\nu$  = kinematic viscosity of water  
 $\rho$  = specific density of water  
 $\phi$  = phase, depending on horizontal coordinate x  
 $\psi = \omega t - \phi(x)$

subscript "o" refers to deep water value.

subscript "1" or "2" refers to first or second harmonic component, respectively.

subscript "h" refers to value on horizontal bottom.

subscript " $\infty$ " refers to value just outside the boundary layer.

References

- (1) - Longuet-Higgins, M.S., "Mass transport in water waves", Phil.Trans. Roy.Soc.London, A., No.903, Vol.245, pp.535-581, 1953.
- (2) - Mei, C.C., Liu, P.L.F. and Carter, T.G., "Mass transport in water waves; Theory and Experiments", M.I.T. Dept.Civil Eng., Ralph M. Parsons Lab.Report No.146, 1972.
- (3) - Russell, R.C.H. and Osorio, J.D.C., "An experimental investigation of drift profiles in a closed channel", Longuet-Higgins, M.S., "The mechanics of the boundary layer near the bottom in a progressive wave", Proc.6th Conf.on Coastal Eng., Chap.10, pp.171-193, 1958.
- (4) - Brebner, A., Askew, J.A. and Law, S.W., "The effect of roughness on the mass transport of progressive gravity waves", Proc.10th Conf.on Coastal Eng., Chap.12, pp.175-184, 1966.
- (5) - Noda, H., "On the oscillatory flow in turbulent boundary layers induced by water waves", Bull.Disas.Prev.Res.Inst., Kyoto Univ., Vol. 20.Part 3, No.176, pp.127-144, 1971.
- (6) - Johns, B., "On the mass transport induced by oscillatory flow in a turbulent boundary layer", Journ.of Fluid Mech., Vol.43, Part 1, pp.177-185, 1970.
- (7) - Sleath, J.F.A., "A second approximation to mass transport by water waves", Journ.of Mar.Res., 30 (3), pp.295-304, 1972.
- (8) - Sleath, J.F.A., "Mass transport in water waves for very small amplitude", Journ.of Hydr.Res.11, No.4, pp.369-383, 1973.
- (9) - Lau, J. and Travis, B., "Slowly varying Stokes waves and submarine longshore bars", Journ.of Geophys.Res., Vol.78, No.21, pp.4489-4497, 1973.
- (10) - Schlichting, H., "Boundary layer theory", Sixth Edition, 1966.
- (11) - Batchelor, G.K., "An introduction to fluid dynamics", Cambridge University Press, 1967.

=====